Online Muon Reconstruction in the ATLAS Muon Spectrometer at the Level-2 stage of the Event Selection

Alessandro Di Mattia on behalf of the ATLAS Collaboration

***Abstract*–To cope with the 40 MHz event production rate of LHC, the ATLAS experiment uses a multi level trigger architecture that selects events in three sequential steps, increasing the complexity of reconstruction algorithms and accuracy of measurements with each step. The Level-1 is implemented with custom hardware and provides a first reduction of the event rate to 75KHz, identifying physics candidates within a small detector region (Region of Interest, RoI). The higher trigger levels, the Level-2 and the Event Filter, are running on dedicated PC farms where the event rate is further reduced to O(400) Hz by software algorithms. At Level-2, the selection of the muon events is initiated by the "MuFast" algorithm, which confirms the muon candidates by means of a precise measurement of the muon candidate momentum. Designed to use a negligible fraction of the Level-2 latency, this algorithm exploits fast tracking and Look Up Table (LUT) techniques to perform the muon reconstruction with the precision muon chamber data within the RoI. The quality of the track parameters is good and approaches that of the offline reconstruction in some detector regions, and enables Level-2 to achieve a significant reduction of the event rate. This paper presents the current state of the art of the L2 algorithm "MuFast" reviewing its performance on the event selection, and the algorithm optimization achieved by using data taken in 2010.**

ATL-DAQ-PROC-2011-039
21 November 2011

I. Introduction

THE ATLAS [1] experiment aims to explore the High Energy Physics frontier at the Large Hadron Collider (LHC), a machine delivering proton-proton collision which are expected to reach a center of mass energy of 14 TeV and a peak luminosity of 10^{34} cm^{-2} s^{-1}. In the LHC, high intensity beam bunches are circulated with a 25 ns time spacing and multiple interactions happen at every bunch crossing with a frequency of 40 MHz. Due to the limited capacity of the storage system and of the offline computing, the huge event rate must be reduced online by five orders of magnitude. This is the challenging task of the Trigger and DAQ system, which is required to implement highly selective algorithms for identifying the interesting physics over a background several order of magnitude bigger. Among the trigger subsystems the one based on muon identification and reconstruction is particularly important because it allows the efficient selection of the promising channels for the Higgs search (e.g. $H\rightarrow WW\rightarrow\mu\mu\nu\nu$, $H\rightarrow ZZ\rightarrow 4\mu$) and of many discovery channels of new physics.

Manuscript received November 15, 2011.

A. Di Mattia is with the Michigan State University, Department of Physics and Astronomy, East Lansing, MI 48824-2320 USA, now at University of Wisconsin (telephone: +41 22 767-8876, e-mail: dimattia@cern.ch).

II. The ATLAS Muon Spectrometer

The ATLAS Muon Spectrometer uses three air core toroidal magnets (one for the barrel and two for the endcaps), that deliver a field of 0.5 T covering the rapidity range up to $|\eta| = 2.7$. Within the magnetic volume are housed planes of tracking chambers arranged in 16 physics sectors having an octant symmetry in the transverse view. Fig. 1 shows the spectrometer layout in the longitudinal view (r, z) that is orthogonal to the magnetic field. The layout of the measurement stations is shown in Fig. 1 and allows for a total lever arm ranging from 5 m to 7 m. The track bending is measured with a precision of 120 μm by the Monitored Drift Tube (MDT) [2] detector. In the innermost station at very large rapidity ($\eta \geq 2$), where the background conditions are extreme (the expected hit rate at the peak LHC luminosity is about 3 KHz/cm^2), the MDT are replaced by the Cathode Strip Chambers (CSC) [2] which allows to reach a precision of 90 μm on a single point measurement. In order to perform the identification of the muon, planes of dedicated trigger detectors are placed near the MDT. They have a fast time response for track hits, required for the bunch crossing identification, and allow for measuring the second coordinate with a mean precision of 1 cm. Two different trigger detector technologies are used: the barrel is equipped with Resistive Plate Chamber (RPC) [3] detectors which have an intrinsic time resolution of ~2 ns, while the endcaps use Thin Gap Chamber (TGC) [4] detectors; compared to the RPC, the TGC has worse time resolution (~10 ns) but provides better efficiency at very high hit rate thus increasing the robustness of the trigger system at large rapidity. Apart from the structure supporting the spectrometer and the services for the detectors, there is no dead material in the spectrometer volume. This allows for a good muon momentum resolution, even at the high energy scale (~1 TeV), with constant performance up to $|\eta| \leq 2.7$.

III. The ATLAS Trigger and DAQ System

The ATLAS experiment selects the physics event with a three-level trigger strategy. The Level-1 trigger [5] searches for muon tracks and calorimeter energy deposits whose transverse momentum and transverse energy is above a given threshold. In order to cope with the very short latency time of 2.5 μs, custom hardware processors are exploited to perform a synchronous parallel analysis of the trigger tower data (i.e. a subset of the detector data providing low resolution measurements) of the Calorimeter and of the Muon

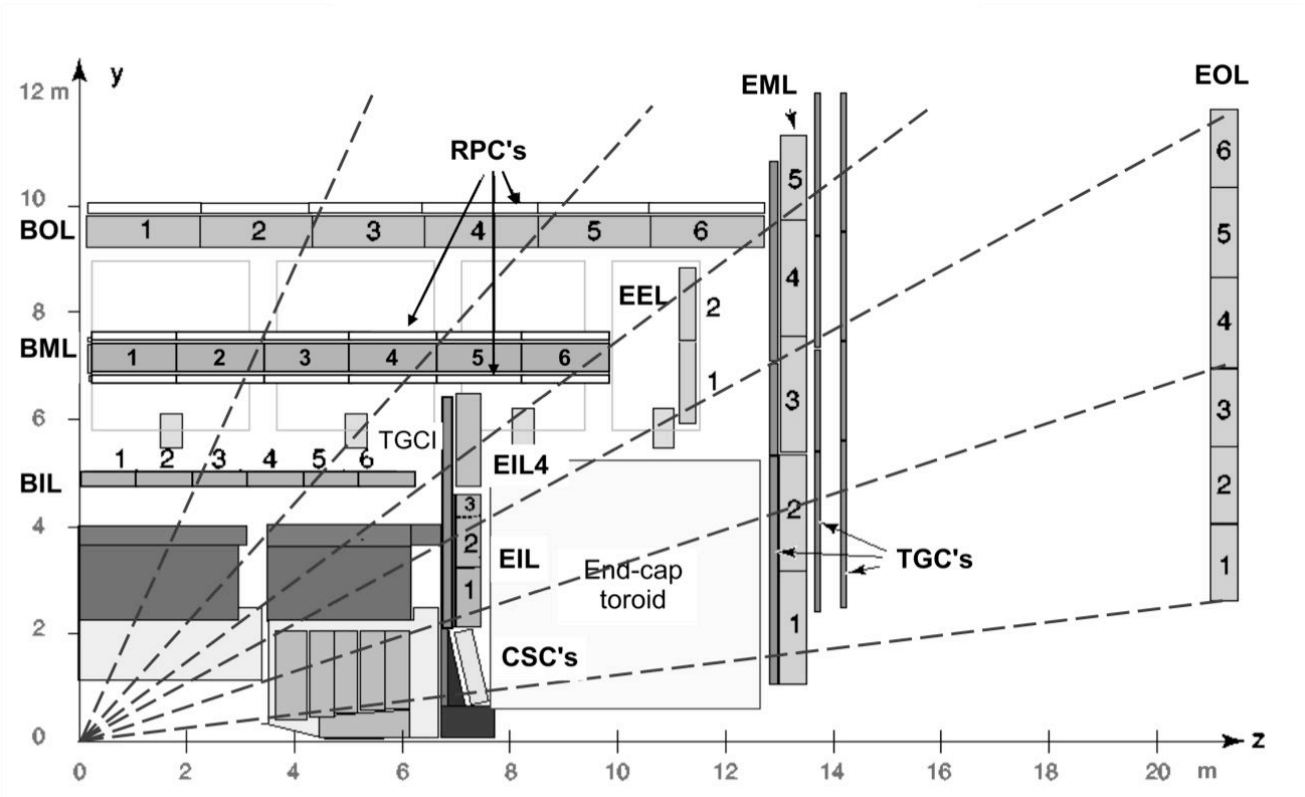

Fig. 1. Longitudinal view of the ATLAS muon spectrometer, showing the MDT stations (BIL, BML, BOL for the barrel, and EIL, EML, EOL for the endcap), the trigger chambers (RPCs for the barrel and TGCs for the endcap) and the CSCs in the very forward region. The dashed lines show the segmentation of the MDT readout into the Read Out Buffer (ROB). The segmentation of the RPC and TGC readout is the trigger sector, which, along the longitudinal view, is made of the full set of chambers shown.

Spectrometer. Although this design limits the accuracy of the event reconstruction, the first trigger level can reduce the input rate of 40 MHz to a maximum output rate of 75 KHz. For the accepted event, the Level-1 identifies the bunch crossing and the detector region (Region of Interest, RoI) where the trigger has fired. After the initial selection the events undergo a software based event selection, called High Level Trigger (HLT) [6], which is implemented by two dedicated processing farms. The Level-2 trigger uses fast reconstruction algorithms to refine the physics properties of the Level-1 candidates, accessing only data from the RoI regions, in a mean latency time of 40 ms. The better energy and track transverse momentum measurements together with the reconstruction of additional properties, such as track isolation, tau identification, b-tagging and jet reconstruction, allow for tighter topological cuts which provide a global reduction factor of about 30 on the input Level-1 rate. At the last selection stage (Event Filter) offline-like algorithms are exploited and the accuracy of the reconstruction is limited only by the non optimal knowledge of the detector condition data (e.g. alignment and calibration constants). Full event data access is also possible which allows for the reconstruction of physics objects that escaped the Level-1 trigger. The increased accuracy of the reconstruction allows to further reduce the event rate to ~400 Hz with a mean latency time of 4 s.

Fig. 2 shows the architecture of the ATLAS Trigger and DAQ system. After being digitized, the detector data are stored in pipeline memories, put in the front-end electronics, to wait for the Level-1 decision. If the event is accepted, the data are transferred into de-randomizer memories, then are sent through the Read Out Drivers (ROD) to the Read Out Buffers (ROB). The ROB concentrates data coming from detector slices arranged in towers projective towards the interaction vertex (Fig. 1 shows the segmentation of the MDT read out). Commodity PCs, the Read Out System (ROS), host the ROBs and serve the event data to the High Level Trigger components. These components are all implemented by means of software programs that run on commodity PCs interconnected with a network to exchange the event data. The Level-2 Processing Unit (L2PU) is the software application responsible for the Level-2 selection. It has the event assigned by the Level-2 Supervisor (L2SV) and requests the ROB data associated with the event RoIs to steer the selection algorithms according to the trigger menu. The network setup connects each Level-2 processing node (currently ~ 800 nodes with 8 cores) to the ROS system; one L2PU runs on each CPU core and has dedicated connection ports assigned to perform the ROB request. The RoI-based access requires only ~2% of the event data, thus limiting the required bandwidth of the dataflow from the ROS to the Level-2 farm. To transfer the full event to the Level-2 farm would have required a data throughput that reaches the limit of the current commercial equipment.

At the Event Filter stage the stability of the dataflow is endorsed by limiting the network connection towards the processing farm. For this purpose, the Event Filter farm is partitioned and the full event data are distributed to the trigger components that process it, rather than being stored in a

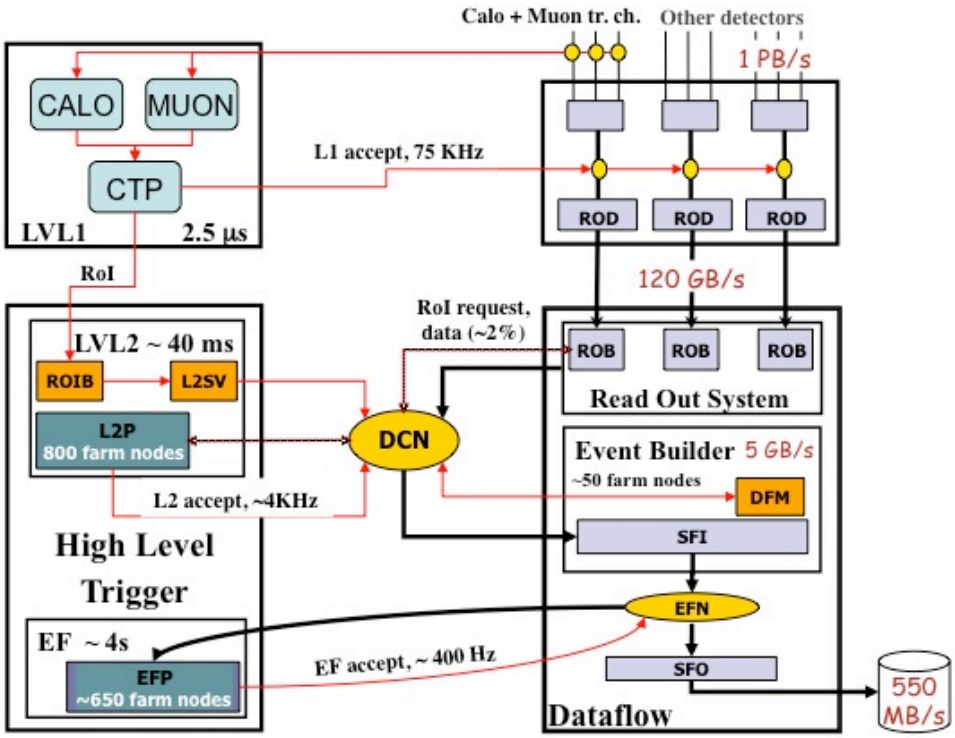

Fig. 2. Schematic diagram of the ATLAS Trigger and DAQ System.

central buffer system as for the Level-2. In the case of a "Level-2 accept" the ROS event fragments and the Level-2 result are sent to the Sub Farm Input (SFI) under the supervision of the Data Flow Manager (DFM). The SFI builds the full event and assigns it to a processing node inside the corresponding Event Filter partition. Here the Event Filter Processing Task (EFPT) (as for Level-2, there is one EFPT per CPU core of the node) performs the final event selection and categorizes the event topology. The accepted event is transferred to the Sub Farm Output (SFO), where, according to its type, is assigned to one of several data stream and sent to the permanent storage.

IV. The Level-2 Muon Trigger

The inclusive search for prompt muons is crucial for many interesting physics processes: low p_T muons are used to perform the flavor tagging of B mesons, whilst high p_T muons are used to reconstruct the decays of heavy objects (e.g. Higgs) and to identify the presence of W, Z, t. At LHC, the background to the prompt muon consists of inflight muon decays of π/k, in the low-p_T spectrum, and the semileptonic muon decay of b, c quarks, in the high-p_T spectrum. Although the production cross sections of these processes have different shapes, they all decrease exponentially with increasing transverse muon momentum. In order to reduce the background contamination to prompt muon, the inclusive muon trigger must have a very sharp p_T threshold.

The Level-1 muon trigger logic identifies the prompt muons hits, in the planes of the RPC and the TGC chambers, with a coincidence window applied on both the hit time and the hit position. To account for the track bending, thus selecting the muon with a p_T threshold, the size of the space coincidence window is programmable, but the design resolution of the trigger chambers limits the sharpness of the Level-1 turn-on curve. Therefore, at Level-2, the full detector data associated with the muon RoI are used to reconstruct the muon. This is accomplished by software algorithms that performs different reconstruction tasks: first the muon track p_T is estimated using only the Muon Spectrometer data (standalone reconstruction, MuFast algorithm), then the Inner Detector data are exploited to further refine the muon track parameters (combined reconstruction, MuComb algorithm) and finally the calorimeter data are processed to check if the muon track is isolated (isolation, MuIso algorithm). Selection cuts on the muon properties are applied after each algorithm execution, in order to stop using the Level-2 resources as soon as it is recognized that the RoI has to be rejected ("early rejection"). In order to save resources it is crucial that the first algorithm executed in the muon selection sequence provides a considerable reduction of the Level-1 rate using a negligible fraction of the Level-2 latency.

V. MuFast

The task of MuFast is to confirm the Level-1 muon candidate by means of a more precise muon momentum measurement (*muon feature extraction*) and to reject the Level-1 fake rate induced by physics background. The better quality of the momentum measurement allows for a sharper p_T threshold, but the short Level-2 latency time (40 ms) demands to use a fast feature extraction method and to perform the RoI data access within a few milliseconds. This latter requirement is crucial for the overall optimization of the trigger latency, because to

move the data from the ROSes can take a big fraction of the latency time (the time for transferring one ROB to the L2PU is about 1 ms).

The need to optimize the data access time at Level-2 has also driven the design of the muon dataflow, which is organized in such a way as to minimize the traffic towards the trigger processors. As shown in Fig. 1, the MDT detector readout is subdivided into projective towers that typically contain two adjacent chambers on each measurement station. Similar schemas are used for the TGC and the RPC data, where the tower consists of the full trigger sector. Data from a single tower flows in one ROB thus increasing the probability to find the muon track data within a few ROBs.

The MuFast algorithm is seeded by the Level-1 RoI consisting of the p_T threshold fired at Level-1 and the $\eta-\phi$ position of Level-1 trigger tower. Because the track bend in the phi projection is negligible in the Muon Spectrometer, the muon can be reconstructed using only the data of one physics sector. To gather the detector data associated with the muon RoI three ROBs are requested: one trigger ROB (either RPC or TGC) and two MDT ROBs corresponding to the towers closest to the RoI in the eta view. This allows the reconstruction of tracks crossing two adjacent towers.

The feature extraction method is the result of an optimization process among the CPU usage and the performance needed to increase the purity of the prompt muon sample: high selection efficiency for high-p_T muons and high rejection of low-p_T muons. The muon track is reconstructed in three sequential steps: a *pattern recognition* that uses the trigger hits to build a seed of the muon tracks then collects the MDT hits found within narrow roads opened along the seed, a *track fit* performed on each MDT station and a *p_T estimate* exploiting a Look Up Table (LUT). The output of the feature extraction is the track position parameters measured at the entrance of the Muon Spectrometer and the muon p_T estimated at the interaction vertex. At this selection stage the interaction vertex is defined as the average position of the interaction provided by the offline measurement.

The advantage of this method is that the LUT p_T estimation does not require to access the magnetic field map and avoid the use of a time consuming minimization procedure. Moreover a pattern recognition not based on combinatorial techniques and disentangled from the fitting procedure allows for tuning the balance among the fake rejection and the track reconstruction efficiency without increasing the demand of CPU power. This is crucial for reaching the optimal plateau efficiency in the spectrometer region where the detector does not have a uniform coverage (mostly in the barrel feet region that hosts the structure supporting the spectrometer and the elevators allowing fast access to the innermost detectors).

This feature extraction method has been initially studied and proposed for the barrel region [7]; the current implementation of the MuFast algorithm uses the same design but adapted to reconstruct also the endcap region.

A. MuFast barrel

In the Muon Spectrometer barrel layout the measurement stations are placed inside the toroidal field. The field intensity is quite homogenous, apart from a periodic variation in phi, and allows for using a constant curvature radius to describe the muon track.

The pattern recognition is seeded by the RPC trigger data. The RPC hit strips (RPC strips read out the induced ionization charge) that fired the trigger logic are identified by input the 16-bit RPC data pattern to an algorithm emulating the Level-1 RPC trigger processor [8]. A circle fit of the RPC hits, constrained with a straight tangent line from the interaction vertex, constitutes the seed of the muon trajectory in the spectrometer. Subsequently, muon roads are opened along the track seed for selecting the MDT muon hits. The road half width is optimized to collect 96% of muon hits for both low-p_T and high-p_T muon trigger; the size ranges from 10 cm in the Large physics sectors (farthest to the barrel coils) to 20 cm in the Small physics sectors (closest to the barrel coils). For the collected hits the residual from the track seed is computed and the outliers are removed in order to reject the hits from the cavern background[1]. Altogether, the MDT hit finding procedure has an efficiency of 96% and a background contamination of 3% (estimated with Monte Carlo and confirmed by observation in the data taking).

To achieve good physics performance for the track measurement, the MDT calibration constants are accessed at runtime for converting the drift time into a space measurement. The drift time measurement requires to subtract from the MDT hit time the muon time-of-flight and the propagation time along the wire, both computed exploiting the second coordinate measured by the RPC. The muon track is approximated with linear segments fit separately on each MDT chamber. A successful fit must have hits on at least 4 MDT layers and provides a precision measurement (*super point*) of the muon track at the middle radius of the MDT station. The Level-1 fake triggers are rejected requiring at least two super points in the event. The curvature radius of the muon track is computed fitting the super points with a circle, as illustrated in Fig. 3;

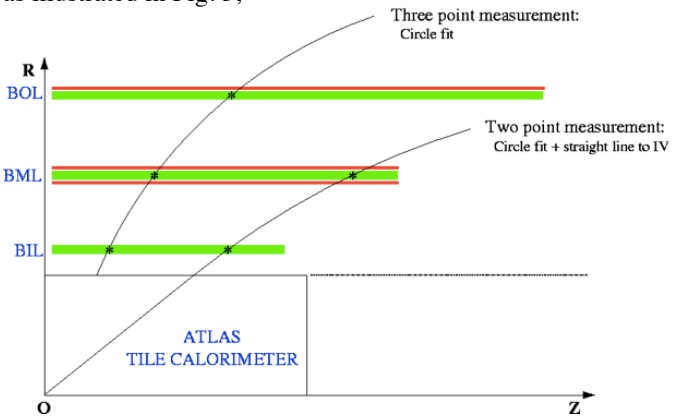

Fig. 3. The method implemented in MuFast to measure the muon track curvature in the barrel of the ATLAS Muon Spectrometer, using the high precision measurement (super points) from the fit of the MDT data.

when only two super points are available the circle is constrained with a straight tangent line from the interaction vertex. Although the measurement of the curvature radius through two super points is subject to a bigger uncertainty, it

[1] The cavern background is constituted of low energy neutrons and photons that leave uncorrelated hits in the muon detector.

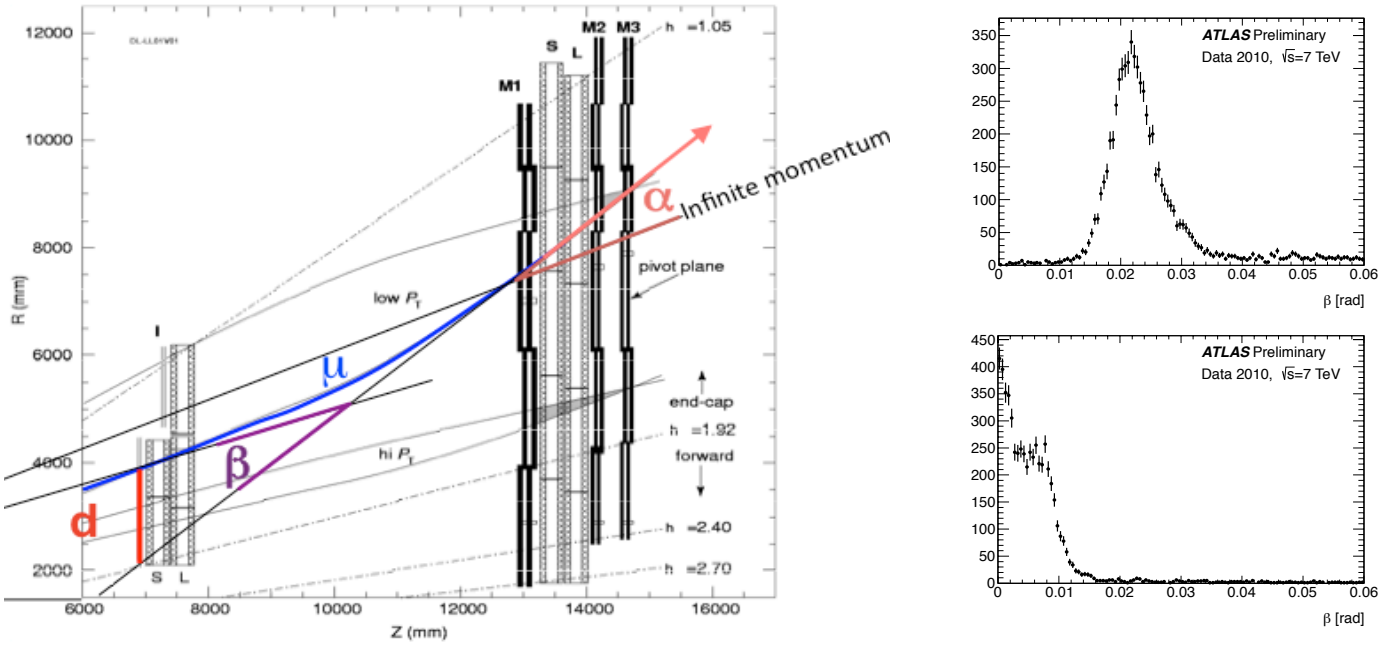

Fig. 4. Left: schema of the ATLAS endcap Muon Spectrometer showing the innermost and middle measurement stations and the quantities (angle *alpha*, angle *beta* and *d*) related to the measurement of the muon momentum. Right top: *beta* distribution for muon track of p_T = 20 GeV in η–ϕ region where the magnetic field is homogeneous. Right bottom: *beta* distribution for muon track of p_T = 20 GeV in η–ϕ region where the magnetic field is highly inhomogeneous (endcap transition region). [11].

allows to reach a very high track reconstruction efficiency (~99%) even in the feet region of the spectrometer barrel.

Finally the muon p_T is estimated using the the linear relationship among the curvature radius and the p_T existing for tracks originating from the interaction vertex

$$r = A_0 \cdot p_T + A_1. \quad (1)$$

This formula has been mapped into a LUT by dividing the detector region in which the algorithm operates into η and ϕ bins and computing the A_0 and A_1 parameters for each bin. The muon track is assigned to a given cell according to its position at the entrance of the spectrometer. The main source of uncertainty on the p_T estimate provided with this method are the multiple scattering at the external surface of the calorimeter, the energy loss fluctuations and the non uniformity of the magnetic field. They all depend on the muon path in the spectrometer, thus the LUT binning has been optimized to minimize these contributions. A binning of 30 cells in η and 30 cells in ϕ is adequate to calibrate the muon reconstruction inside a physics sector of the spectrometer. The effect of the finite size of the LUT is rendered less important through the use of an interpolation procedure.

B. MuFast endcap

In the Muon Spectrometer endcap layout the measurement stations are placed outside the toroidal field. In contrast to the barrel, the intensity of the magnetic field is highly inhomogeneous, especially in the endcap transition region due to the interference among the barrel and endcap coils. As a consequence the muon track cannot be described by a constant curvature radius and requires a different model to estimate the p_T. As illustrated in Fig. 4, the muon track slope can be fit before the toroidal bending (inner slope, fit in the Innermost station) and after the toroidal bending (middle slope, fit in the Middle station). Two quantities are used for building the LUT to estimate the muon p_T: the angle *alpha* between the middle slope and the direction of the infinite momentum track, and the angle *beta* between the inner slope and the middle slope. The *beta* measurement allows for the best resolution on the muon p_T, but the *alpha* measurement provides the best efficiency for the track reconstruction, because only the middle slope is needed. In the region where the magnetic field is highly inhomogeneous both *alpha* and *beta* are not well defined, as is shown for *beta* in Fig. 4, thus causing big uncertainty on the p_T estimation. Therefore the p_T resolution achieved with the LUT method in the endcap is worse than the barrel one.

The TGC hits that contributed to the Level-1 decision are available in the readout data and input to a linear fit that estimates the muon track slope (TGC slope) in the Middle station. This allows for a first estimation of the muon p_T with the *alpha* measurement and constitutes the seed for the MDT pattern recognition. The muon MDT hits in both Middle and Outer stations are efficiently selected by a 10 cm half width road opened around the TGC slope. In order to use the same road size for the Innermost station the track is back-extrapolated through the magnetic field. For this purpose a LUT storing the shift *d* (see Fig. 4) from the TGC slope as a function of the track p_T is used. Thanks to the use of narrow roads in the Innermost station, the MDT hit finding procedure has a background contamination lower than 5% (estimated with Monte Carlo and confirmed by observation in data taking).

As for the barrel, the MDT data are fit together to build linear segments on each MDT station that measure the track slope. If the segment in the Outer station is available (the endcap Outer station covers only the rapidity range from η=1.5 to η=2.5) it is combined with the segment in the Middle station to provide

a more precise measurement of the track slope after the magnetic bending. Using the track slopes the angles *alpha* and *beta* are reconstructed.

To estimate the muon p_T the quadratic relationships

$$alpha = A_\alpha \cdot \frac{1}{p_T} + B_\alpha \cdot \left(\frac{1}{p_T}\right)^2 \quad , \qquad (2)$$

$$beta = A_\beta \cdot \frac{1}{p_T} + B_\beta \cdot \left(\frac{1}{p_T}\right)^2 \quad ,$$

are preferred, because the linear formulas yield a systematic shift, dependent on the momentum range, on the estimated p_T. Both LUT for alpha (αLUT) and LUT for beta (βLUT) are computed. For a track with p_T lower than 8 GeV the estimation from the αLUT has the same resolution of the estimation from the βLUT; the *alpha* measurement has better reconstruction efficiency thus it is preferred. The higher p_T tracks are better estimated with the βLUT, because it is less affected by the uncertainty originating from the spread of the interaction vertex. A LUT binning of 30 cells in η and 12 cells in φ is adequate to calibrate one endcap physics sector (0 rad < φ < 0.39 rad); a finer segmentation in phi does not improve the modeling in the problematic regions.

C. Online implementation

MuFast runs in the software framework provided by the L2PU [9]. This framework reuses the offline software components in order to allow a transparent running of the trigger algorithm in both online and offline environment. In the MuFast code, the commonalities between the offline and the online software architectures are used to implement the data access, but some of the components have been modified in order to optimize the MuFast latency. In particular the offline tools that access the detector condition data (e.g. geometry, cabling and alignment) have been substituted with Level-2 specific services that provide a faster access time and can serve the data to concurrent event processing threads. Further optimization of the latency has been achieved embedding the MDT data decoding procedure in the algorithm code. This implementation allows for decoding only the MDT hit in the pattern recognition road; in contrast the offline procedure steers the decoding of all the detector chambers associated with the muon RoI, thus adding a big time overhead due to the large chamber occupancy.

The algorithm code has been tested online for the first time at the 2004 ATLAS testbeam on the extraction beam line H8 [7]. Subsequently it was used in several large scale tests to check the dataflow performance and trigger latency. Finally it has been put in operation in the ATLAS pit (point 1) where was commissioned with the cosmic runs [10]. The online processing of the cosmic events allowed for checking the robustness of the code against data corruption, for implementing the monitoring and the error recovery procedures and for validating the pattern recognition of MuFast.

VI. Operation in 2010

In the 2010 data taking campaign MuFast was operated with untuned LUTs because the alignment of the Muon Spectrometer was not available at the beginning and the muon statistics initially delivered by LHC was too low to make a sensible comparison with the Monte Carlo predictions. Moreover the calibration of the Level-1 timing was not optimal causing some RoI from prompt muon to be assigned to a wrong bunch crossing (out-of-time RoI). Being these RoIs not processed by the standard Level-2 muon selection (hence the event is potentially rejected) a modified version of MuFast, able to identify the out-of-time prompt muon with an efficiency of 84%, was put in operation. The recovery of out-of-time muons was crucial for the optimization of the Level-1 timing.

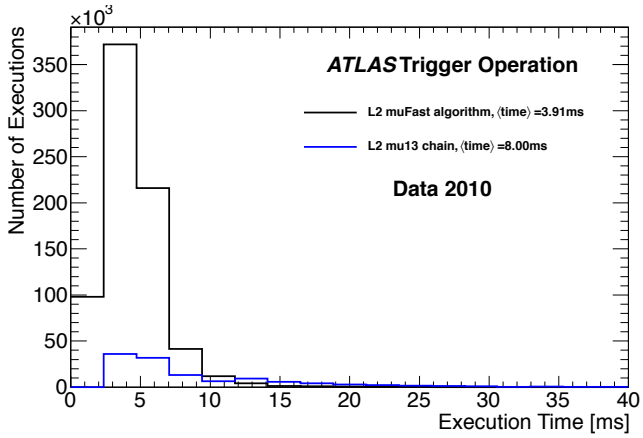

Fig. 5. MuFast online wall-clock time (i.e. including the ROS access and the data transfer time) per RoI. The wall-clock time of the mu13 selection chain, including the Inner Detector tracking and the combined reconstruction algorithm is also shown. [11].

In the muon event selection strategy, MuFast was exploited to collect an unbiased p_T sample of prompt muon by adjusting the thresholds to the lowest value that allowed a sustainable output event rate. Although the p_T cut was not effective, due to the non-tuned LUT, a rate reduction of a factor of 1.6 on the Level-1 input rate has been achieved. This was mostly due to the good performance of the pattern recognition, which rejected the fake triggers from Level-1 (Level-1 was operated with the lowest possible threshold too, in order to increase the efficiency for the *b*-physics channels). Altogether the performance on the track reconstruction (for the in-time muons) was approaching the designed value of 99%.

Fig. 5 shows the online latency time of MuFast measured by the monitoring infrastructure. The pure processing time of the algorithm is about 1 ms while the mean latency for the RoI data access is about 3 ms.

A. Tuning the Look Up Table with 2010 data

After August 2010 the calibration of the Level-1 timing was optimized and the muon statistics in the high-p_T region of the spectrum was slightly improved due to the increase of the LHC luminosity. The alignment of the spectrometer was also computed, thus the event data allowed for the tuning of the MuFast LUT. This work requires the offline reprocessing of the trigger algorithm selection on a sample of prompt muons which are reconstructed using the best knowledge of the spectrometer alignment. The muon p_T spectrum is subdivided into bins of full width of $2{\cdot}\sigma$, being σ the offline resolution for

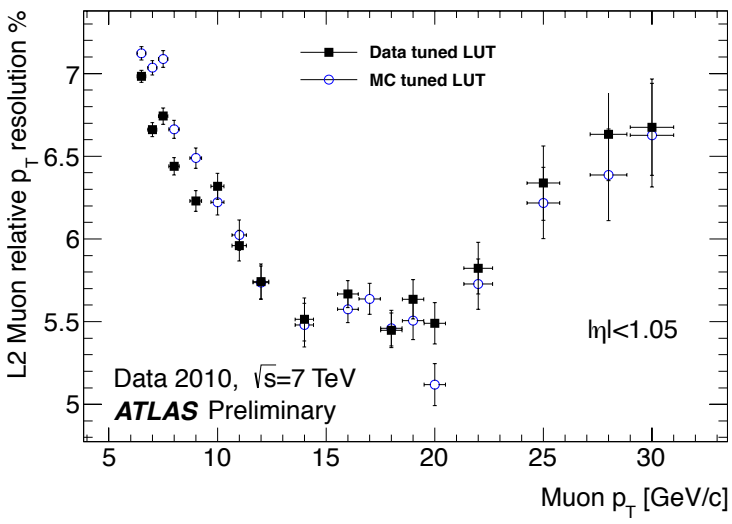

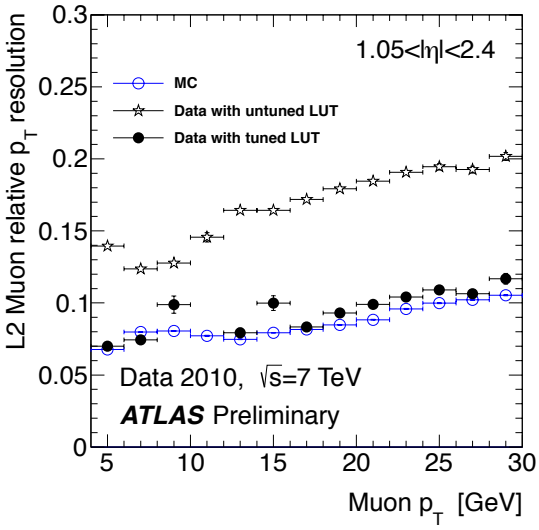

Fig. 6. Left: Relative p_T resolution for the barrel region (|h|<1.05) for 2010 data reprocessed with the Look Up Tables (LUT) for the p_T estimation computed using the best knowledge of the alignment condition data. Right: Relative p_T resolution for the endcap region (1.05<|h|<2.4) for 2010 data reprocessed with te Look Up Tables (LUT) for the p_T estimation computed using the best knowledge of the alignment condition data. [11].

the p_T value at the center of the bin. Events of each p_T bin are assigned to the corresponding LUT bin and the corresponding parameters for the p_T estimation are computed. To achieve a high precision in the tuning, 10^6 events are required into at least two p_T bins. In order to gather the required statistics in a big fraction of the p_T spectrum, a total integrated luminosity of 10 pb^{-1} was reprocessed. This yielded enough statistics at the 6 GeV pT bin, but only ~10^5 prompt muons were reconstructed in the 20 GeV p_T bin. Therefore the tuning for the high-p_T part of the spectrum (greater than 20 GeV) is affected by large statistic uncertainty.

Fig. 6 shows the p_T resolution on 2010 data, achieved after having tuned the LUTs, as a function of the muon p_T. The resolution in the barrel is 7% for a 6 GeV p_T muon and 5.5% for a 20 GeV p_T muon; these values are a factor of about 2 worse than the offline p_T resolution. In the endcap the p_T resolution does not achieve the good performance of the barrel due to the large inhomogeneity of the magnetic field in the transition region: at 6 GeV the resolution is 8% and at 20 GeV the resolution is 9.5%. These results, obtained with the best knowledge of the muon spectrometer condition data, constitute a benchmark for the MuFast performance. Simular result can be achieved from LUT tuned with the Monte Carlo.

VII. Operation in 2011

In the 2011 data taking campaign MuFast uses the LUT tuned with the 2010 data and selects the prompt muon events by setting a sharp p_T threshold. Fig. 7 shows the MuFast resolution as a function of the reconstructed muon p_T measured by the offline data quality procedure. While the resolution for 6 GeV p_T agrees with the benchmark results on 2010 data, the resolution for the 20 GeV p_T muon is slightly worse: in the barrel it is 9% and in the endcap it is 11%. The degradation spot for the high-p_T spectrum can be modeled by summing in quadrature to the benchmark resolution a constant term equal to 6.5% for both barrel and endcap. Such term describes the uncertainty due to the multiple scattering and to

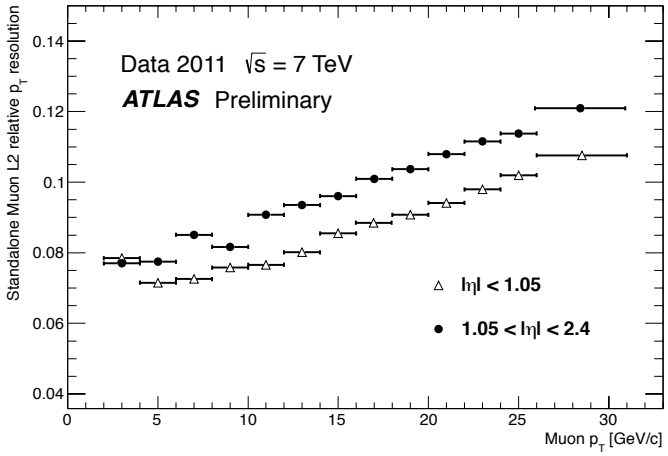

Fig. 7. Relative p_T resolution of MuFast for 2011 data as a function of the reconstructed muon p_T. At high-p_T, the barrel performance is slightly degraded with respect to the tuning. [11].

the spectrometer misalignment. It correspond to an error on the muon sagittal ranging from 1.5 to 2.5 mm which is likely originated by the change in the spectrometer alignment between 2010 and 2011. Notwithstanding the degradation of the p_T measurement, the performance for the prompt muon selection were adequate, so the LUTs have not been retuned.

The selection efficiency for the thresholds at 15 GeV and the 20 GeV is shown in Fig. 8. They have been computed from the di-muon decay of the Z, where one muon is the one that triggers the event and the other is used for probing the selection efficiency for prompt muons (tag and probe method). In the barrel, the inefficiency at plateau is about 2%; 0.7% originates from border effects at the boundaries of the detector coverage (mostly in the feet region), 1.3% originates from readout problems happened in the period considered for this study. In the endcap the inefficiency at plateau is about 4% mostly originated from the non Gaussian tail of the resolution on the p_T measured in the transition regions. In order to limit the impact of such inefficiency, the threshold applied for the

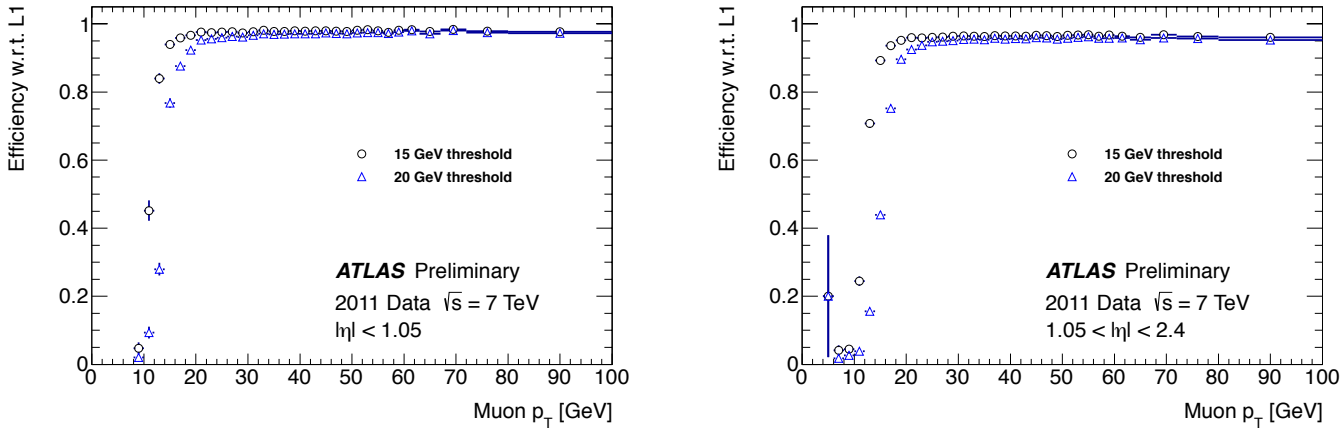

Fig. 6 Left: MuFast turn on curves for the barrel region computed with respect to LVL1. The total 2% plateau inefficiency of MuFast originates from border effect in the feet region (~0.7%) and from bad detector status and/or bad LVL1 timing. Right: MuFast turn on curves for the endcap region computed with respect to LVL1. The total 4% inefficiency of MuFast originates mostly from the large resolution tails in the transition region, where the magnetic is highly inhomogenous due to the interference among the barrel and the endcap toroids. [11].

high-p_T selection is 6 GeV because it allows for an higher plateau efficiency (~97.5%). The correct p_T selection is applied after the combined reconstruction.

Altogether MuFast reduces the Level-1 input rat by a factor of 2. Table 1 shows the reduction factors to the Level-1input rate observed online.

TABLE I. OBSERVED RATE REDUCTION FACTORS FOR THE LEVEL-1 INPUT RATE FROM DIFFERENT THRESHOLDS

Level-1 input theshold	Reduction factor
4 GeV	2.2
6 GeV	1.6
10 GeV	3.3
15 GeV	2.7
20 GeV	2.4

VIII. CONCLUSIONS

The Level-2 algorithm MuFast is currently operated in ATLAS High Level Trigger and contributes to the prompt muon selection. Thanks to the tuning of the LUTs, made with the 2010 data, the algorithm reduces input Level-1 rate by a factor of 2 using only 10% of the full Level-2 latency time. The performance for the prompt muon selection matches these of the design study. The algorithm provides good robustness and high responsiveness when operated under non optimal condition of the Level-1 trigger; this ensures that MuFast will be adequate to cope with the increase of the luminosity foreseen the next year.

REFERENCES

[1] ATLAS Collaboration, "ATLAS Technical proposal for a general-purpose PP experiment at the large hadron collider at CERN," CERN/LHCC/94-4, 1994.

[2] ATLAS Collaboration, "ATLAS Muon Spectrometer Technical Design Report," CERN/LHCC/97-22, 1997.

[3] R. Santonico, "Topics in resistive plate chambers," *Scientifica Acta*, vol. 11, p. 1, Jun. 15, 1996.

[4] [4] Y. Ari, "Thin gap chamber: Performances as a time and position mea- suring device," *Scientifica Acta*, vol. 11, p. 349, Jun. 15, 1996.

[5] ATLAS Collaboration, "ATLAS Level-1 Trigger Technical Design Report," CERN/LHCC/98-14, 1998.

[6] ATLAS Collaboration, "ATLAS High-Level Trigger Data Acquisition and Controls Technical Design Report," CERN/LHCC/2003-022, 2003.

[7] A. Di Mattia et al. , "Online Muon Reconstruction in the ATLAS Level-2 Trigger System", *IEEE Trans. Nucl. Sci.*, vol. 53, n. 3, pp. 1339-1346, Jun. 2006

[8] V. Bocci, E. Petrolo, A. Salamon, R. Vari, and S. Veneziano, "The coincidence matrix ASIC of the Level-1 muon barrel trigger of the ATLAS experiment," *IEEE Trans. Nucl. Sci.*, vol. 50, no. 4, pp. 1078–1085, Aug. 2003.

[9] W. Wiedenmann, "Studies for a common selection software environment in ATLAS: From level-2 trigger to offline reconstruction," *IEEE Trans. Nucl. Sci.*, vol. 51, no. 3, pp. 915–920, Jun. 2004.

[10] A. Di Mattia on behalf of the ATLAS Collaboration, "Commissioning of the ATLAS High Level Trigger with Single Beam and Cosmic Rays", *Journal of Physics*: Conference Series 219 (2010).

[11] ATLAS Experiment - MuonTriggerPublicResult, https://twiki.cern.ch/twiki/bin/view/AtlasPublic/MuonTriggerPublicResults, accessed 15/11/2011.